Science of Sintering, **39** (2007) 229-240

doi: 10.2298/SOS0703229I

UDK 662.785:661.847.2:57.012.3

Influence of Bi_2O_3 on Microstructure and Electrical Properties of ZnO-SnO_2 Ceramics

T. Ivetić[1*)], M. V. Nikolić[2], M. Slankamenac[3], M. Živanov[3], D. Minić[4], P. M. Nikolić[5], M. M. Ristić[5]

[1]Institute of Technical Sciences of the Serbian Academy of Sciences and Arts, Knez Mihailova 35/IV, 11000 Belgrade, Serbia

[2]Center for Multidisciplinary Studies of the University of Belgrade, Kneza Višeslava 1, 11000 Belgrade, Serbia

[3]Faculty of Technical Sciences, University of Novi Sad, Trg Dositeja Obradovića 6, 21000 Novi Sad, Serbia

[4]Faculty of Physical Chemistry, University of Belgrade, Studentski trg 12-16, 11000 Belgrade, Serbia

[5]Serbian Academy of Science and Arts, Knez Mihailova 35, 11000 Belgrade, Serbia

Abstract: *The effects of small amounts (0.5; 1.0 and 1.5 mol. %) of bismuth oxide on the microstructure and electrical properties of ZnO-SnO_2 ceramics have been studied. Starting powders of ZnO and SnO_2 were mixed in the molar ratio 2:1. After adding Bi_2O_3 this mixture was mechanically activated for 10 minutes in a planetary ball mill, uniaxially pressed and sintered at 1300ºC for 2h. The phase composition of the sintered samples was analyzed by X-Ray Diffraction (XRD) and by Energy Dispersive Spectrometer (EDS). Morphologies were examined by Scanning Electron Microscopy (SEM). An Impedance/Gain Phase Analyzer (HP 4194A) was used to measure the impedance spectra (100Hz – 10MHz) at different temperatures. The electrical DC resistivity/conductivity at different temperatures was measured using a High Resistance Meter (HP 4329A).*

Keywords: *Electrical Properties, Microstructure, Zinc Stannate, and Sintering*

Introduction

In the past decade intense research has been performed on the ZnO-SnO_2 system especially regarding the synthesis of zinc stannate (Zn_2SnO_4). Zinc stannate belongs to the A_2BO_4 spinel type compounds (A = group II, e.g. Zn, B = group IV, e. g. Sn, Ge) [1]. Several types of bulk and thin film materials containing polycrystalline zinc stannates were obtained as potential materials for gas sensing and detection of moisture, as electrodes for solar batteries and in transparent electronics [2-4], etc.

The idea of doping ZnO-SnO_2 based ceramics with Bi_2O_3 as a sintering promoter lies in the fact that the presence of Bi_2O_3 creates conditions for liquid phase sintering. Bismuth oxide forms the $Bi_2Sn_2O_7$ pyrochlore phase with SnO_2 and with addition of ZnO leeds to the formation of Zn_2SnO_4 spinel and a Bi_2O_3 liquid phase between 1000º and 1100ºC, according

*) Corresponding author: tamara@itn.sanu.ac.yu

to the following reaction [5]:

$$Bi_2Sn_2O_7 + 4ZnO \xrightarrow{1000^\circ - 1100^\circ C} 2Zn_2SnO_4 + Bi_2O_3\ (l). \qquad (1)$$

This liquid phase-assisting mechanism is assumed to be the main cause of enhancement of the densification process in the case of sintering with small additions of Bi_2O_3 [6]. The base system mixture ($2ZnO\text{-}SnO_2$) grains get completely surrounded by a thin film of liquid Bi_2O_3, which directly influence the densification process, grain growth and solid-state reaction between attendant ZnO and SnO_2 grains.

This work is an attempt to create a better understanding of the microstructural evolution in the $ZnO\text{-}SnO_2$ system and characterization of its electrical properties when low amounts of bismuth dopant are employed and the samples were prepared by the mixed oxide route. The Mott model was taken into account while fitting the experimental DC conductivity results and investigating the conduction mechanism of sintered samples. This study should lead to establishing the minimum doping level required to optimize both the sintering process and microstructure evolution in Bi_2O_3 doped $ZnO\text{-}SnO_2$ ceramics.

Experimental

Commercially available zinc oxide (Aldrich) and tin oxide (Aldrich) powders were mixed in the 2:1 molar ratio. After adding different amounts of Bi_2O_3 (0.5; 1.0 and 1.5 molar %) this mixture was homogenized in absolute ethanol, dried at 70ºC and mechanically activated in a planetary ball mill (Fritsch Pulverisette 5) for 10 min. Zirconium oxide grinding balls (10 mm in diameter, approx.) and vessels (500 cm^3) were used. The powder to balls ratio was 40:1 and the total weight of the powder mixtures was 15 g. These samples were then uniaxially pressed under 980 MPa into discs with a diameter of 10 mm and ~2 mm thickness.

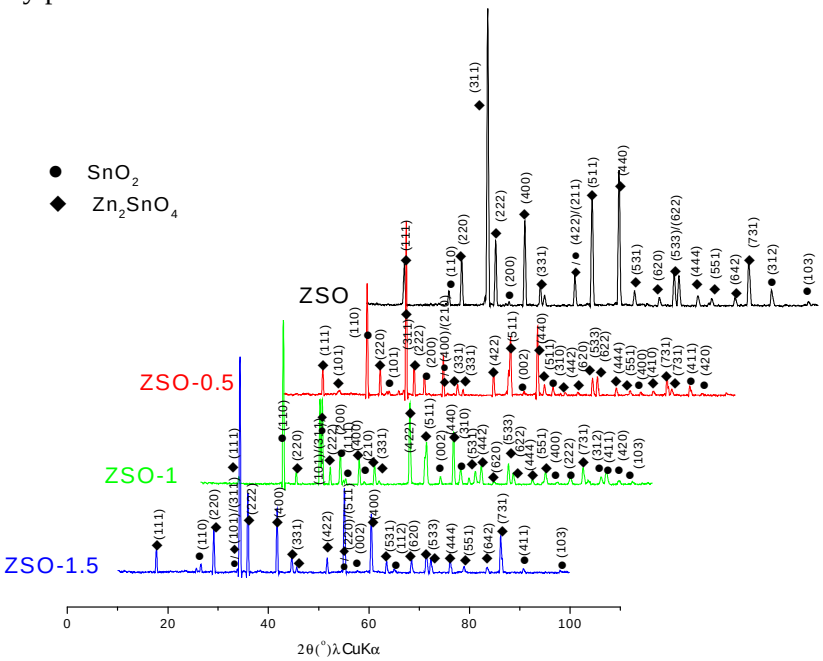

Fig. 1 X-ray diffraction patterns of sintered samples.

Characterization of the obtained samples after sintering was carried out using an X-ray diffractometer (Norelco-Philips PW-1050) with CuK_α radiation and a step scan mode of

0.02º/0.4s. The microstructure of sintered samples was investigated using scanning electron microscopy (SEM – JEOL JSM 6460LV). Appropriate samples were denoted as: ZSO-0.5, ZSO-1.0 and ZSO-1.5, for samples with addition of 0.5, 1.0 and 1.5 molar% of Bi_2O_3, respectively. The reference powder mixture, with no addition of Bi_2O_3 denoted as ZSO, was also prepared using the same procedure.

The samples used for electrical conductivity measurements were prepared in the form of a sandwich electrode structure. Silver coatings were used as electrodes (ohmic contact). An Impedance/Gain Phase Analyzer (HP 4194A) was used to measure the impedance spectra (100Hz – 10MHz) at different temperatures. The electrical DC resistivity/conductivity at different temperatures was measured using a High Resistance Meter (HP 4329A).

Results and discussion

X-ray diffraction and density-microstructure development study

The X-ray diffraction (XRD) patterns for the sintered samples (Fig. 1) point out the existence of a two-phase system composed of Zn_2SnO_4 and SnO_2 phases. XRD peak intensities and their number changes (increase/decrease) for samples with addition of Bi_2O_3 compared to the peaks of Zn_2SnO_4 and SnO_2 seen in the reference ZSO sample diffractogram. This could indicate initial action in the SnO_2-Zn_2SnO_4 system, where Sn^{4+} from tin dioxide, can substitute Zn^{2+} sites in Zn_2SnO_4 [7], as described by the following equation:

$$SnO_2 \xrightarrow{Zn_2SnO_4} Sn_{Zn}^{2+} + O_2 + 2e^- . \quad (2)$$

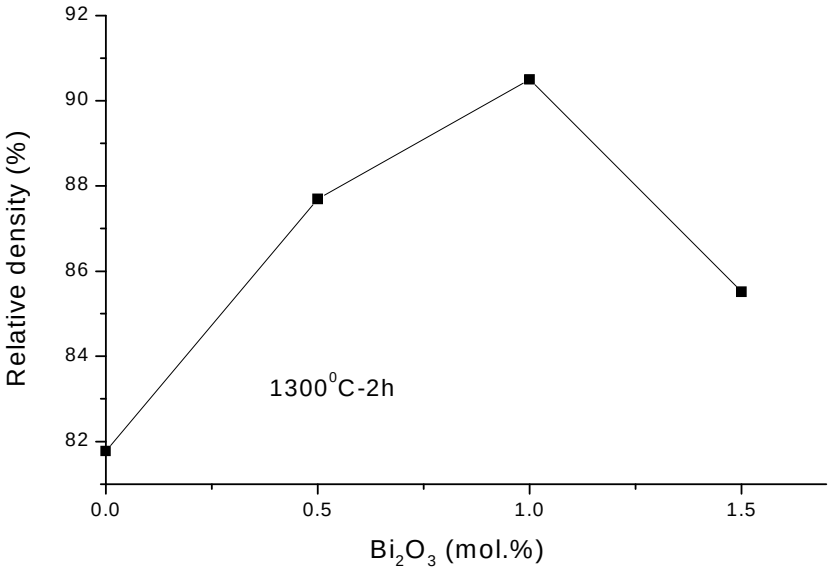

Fig. 2 Sintered density as a function of the Bi_2O_3 content.

From our results it is obvious that small additions of bismuth oxide strongly promote this ion substitution and accelerate the formation of a SnO_2/Zn_2SnO_4 solid solution. However, the XRD study didn't show the presence of free Bi_2O_3 or secondary peak phases, i.e. formation of any new phases. This is because either the added Bi_2O_3 amounts were too small to be detected by X-ray diffraction technique or the applied sintering temperature regime

(1300ºC/2h) created conditions for Bi_2O_3 evaporation*[8].

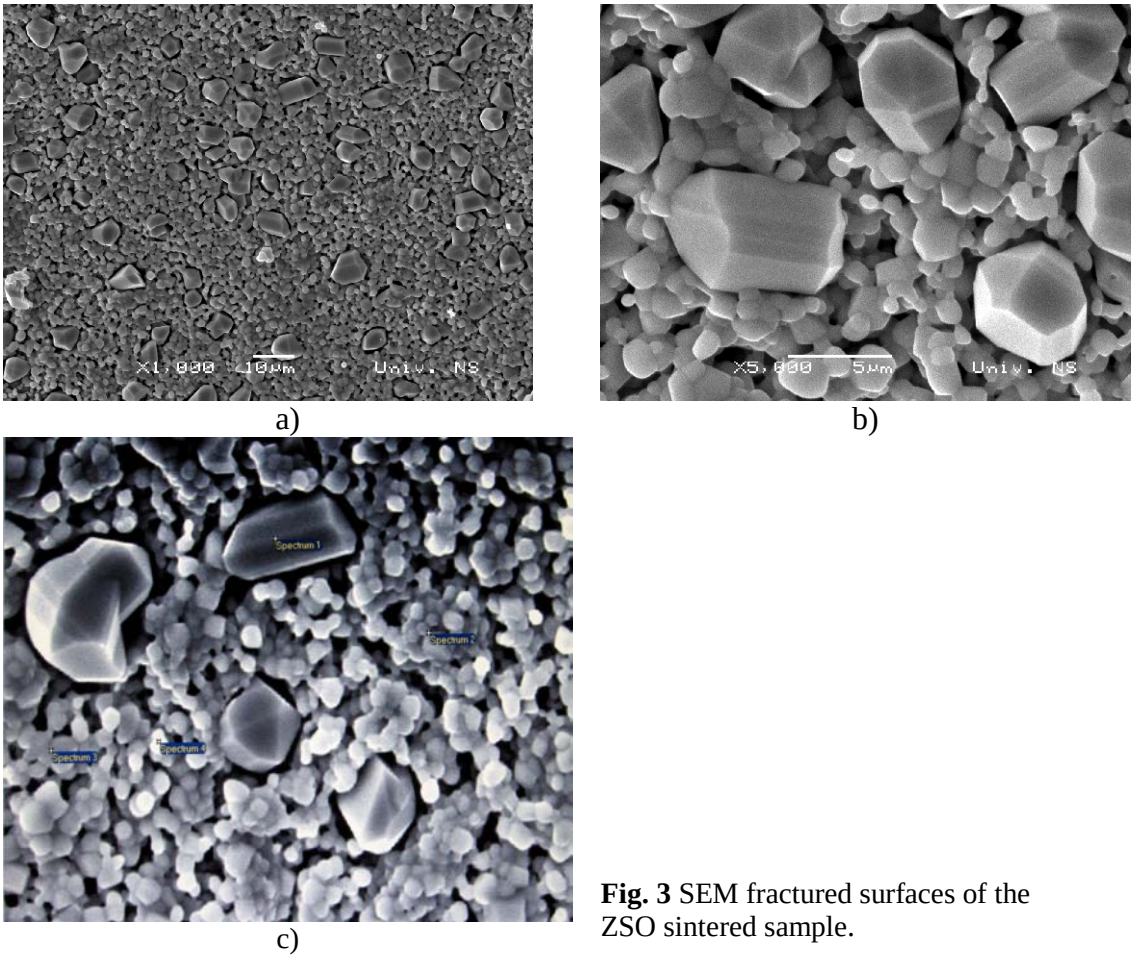

a) b) c)

Fig. 3 SEM fractured surfaces of the ZSO sintered sample.

It is well known that bismuth oxide is used as an obligatory constituent in ZnO commercial varistors and together with minor additions of some other oxides promotes the densification process, influences the formation of a specific microstructure and, consequently impacts the varistor response [9]. By studying the evolution of the sintered densities of the samples as a function of the Bi_2O_3 content (Fig. 2), the effect of Bi_2O_3 addition in enhancing densification of ZnO-SnO_2 ceramics was noted. According to these results the sintered density increases with increasing Bi_2O_3 up to 1.0 molar %. For higher Bi_2O_3 concentration (>1molar%), the sintered density rapidly breaks down as shown in Fig. 2, i.e. indicating the presence of a dedensification phenomenon [10]. So, the optimal amount of Bi_2O_3 to be used as an aid for enhancement of the densification process for sintering 2ZnO-SnO_2 ceramics, is 1.0 molar% in the temperature-time regime of 1300ºC-2h.

The effects of composition on the microstructure was studied with SEM analysis (Fig. 3-6 (a, b)) and with EDS analysis (Fig. 3-6 (c) shows marked points where the EDS measurements where taken, Tab. I). The reference sample has a rather porous microstructure (Fig. 3b) which is dominated by smaller grains with a composition close to the stoichiometric Zn_2SnO_4 spinel-type compound (66% ZnO and 33% SnO_2) and with larger polymeric particles of a secondary SnO_2 phase, incorporated into the spinel structure.

* The final amount of retained Bi is expected to be much smaller, especially knowing the tendency of Bi_2O_3 for evaporation above ~825ºC

Tab. I EDS measurements, (atomic wt%)

Sample	Spectrum	O	Zn	Sn	Total
ZSO	1	81.45	-	18.55	100
	2	70.91	18.90	10.19	
	3	75.51	15.61	8.88	
	4	60.47	26.08	13.46	
ZSO-0.5	1	81.65	11.71	6.64	100
	2	75.88	15.59	8.53	
	3	83.42	-	16.58	
	4	72.23	17.89	9.88	
ZSO-1	1	62.05	-	37.95	100
	2	83.46	-	16.54	
	3	85.17	0.52	14.31	
ZSO-1.5	1	75.20	-	24.80	100
	2	74.46	16.29	9.25	
	3	77.58	14.02	8.39	

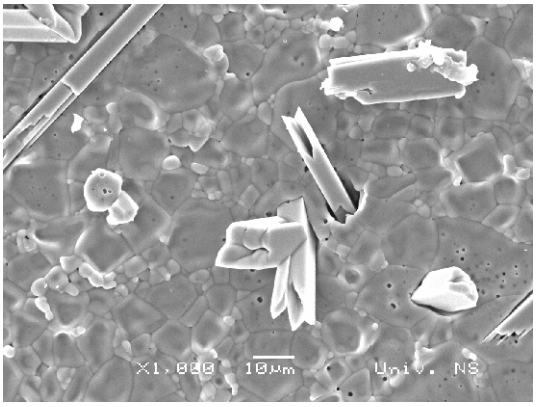

a)

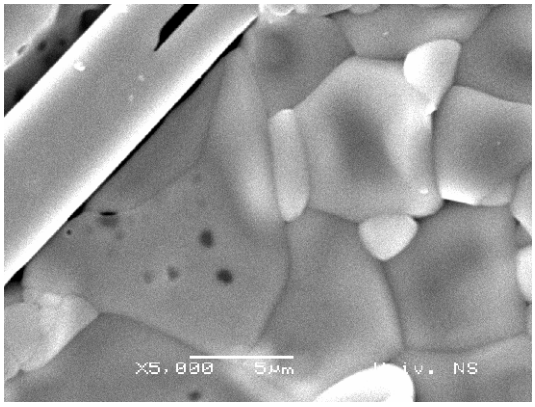

b)

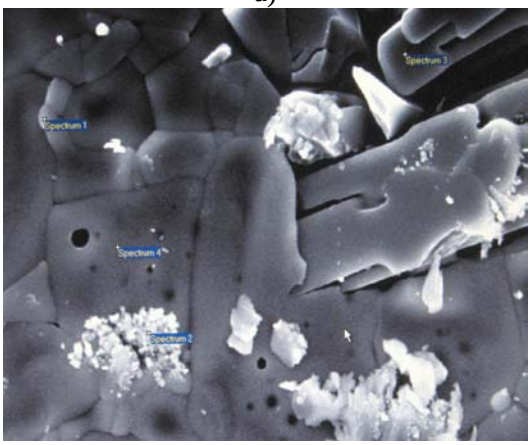

c)

Fig. 4 SEM fractured surfaces of the ZSO-0.5 sintered sample.

The doped sintered samples general microstructure indicates enhancement of the densification process and pinning effect of SnO_2 particles compared to the microstructure of the reference ZSO sintered sample. Processes of densification and grain growth are obvious in the ZSO-0.5 sample (Fig. 4b).

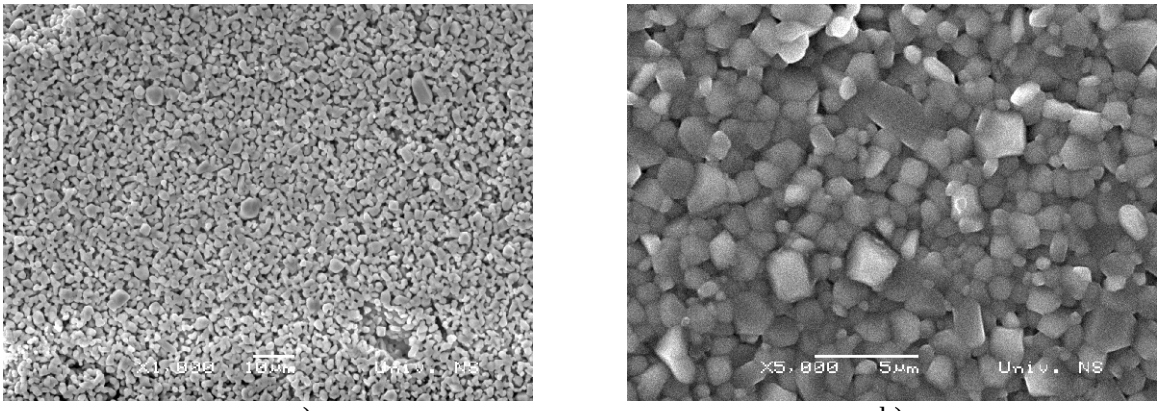

a) b) c)

Fig. 5 SEM fractured surfaces of the ZSO-1 sintered sample.

Equalization of particle sizes occurs in ZSO-1 and the most homogeneous and dense microstructure is formed (Fig. 5b). Further crystal growth and the problem of bigger particle packing in the ZSO-1.5 sample (Fig. 6a-c) cause decrease of the relative density (Fig. 2).

DC conductivity

DC conductivity was analyzed using the Arrhenius equation:

$$\sigma_{DC} = C \exp(-\Delta E/kT), \quad (3)$$

where C is the pre-exponential factor, ΔE is the thermal activation energy, T is the absolute temperature and k is Boltzmann's constant. Fig. 7 shows the variation of DC conductivity (σ_{DC}) with reciprocal temperature (1/T) for the sintered samples. The plot of log (σ_{DC}) versus (1/T) in the temperature range 323-473K, yield a straight [11] line with a slope of –ΔE/k. The activation energies ΔE, calculated from the slope of the straight line and the pre-exponential factors C, obtained by extrapolating the log σ line to the value corresponding to 1/T = 0 [12], are given in Tab. II.

Tab. II Calculated values for ΔE and C from relation (3)

Sample	ΔE (eV)	C $(\Omega cm)^{-1}$
ZSO	1.11	20.2
ZSO-0.5	0.93	10.3
ZSO-1	0.97	10.9
ZSO-1.5	1.16	7.5

It is clear that a small addition of Bi_2O_3 to the ZnO-SnO_2 system has the same influence on electrical characteristics as on the relative density while the thermal activation energy does not show changes which indicates the same conduction mechanism in the whole examined temperature interval.

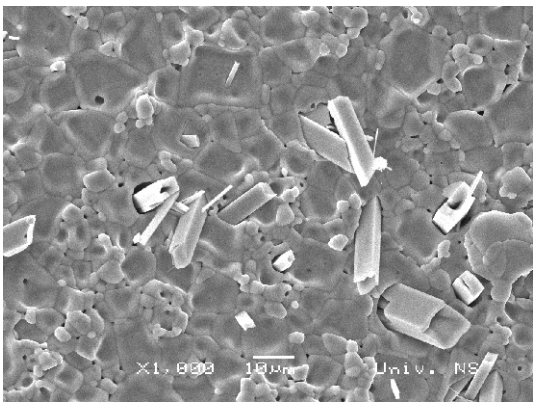

a)

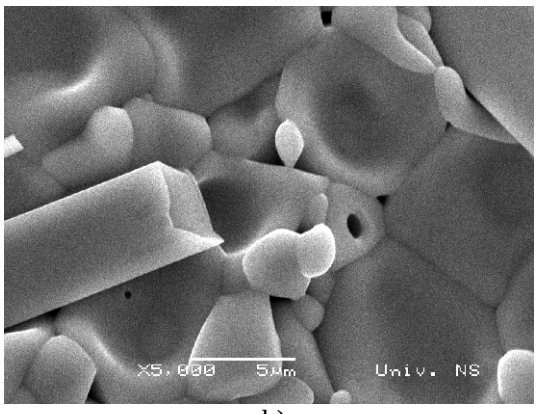

b)

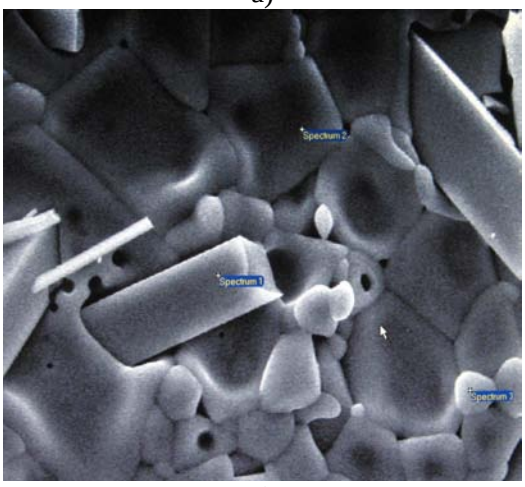

c)

Fig. 6 SEM fractured surfaces of the ZSO-1.5 sintered sample.

According to Fadell et al. [13], the calculated value of ΔE alone does not provide any indication on the conduction mechanism aspects, i.e. whether conduction occurs in the extended states above the mobility edge or by hopping in the localized states.

Mott [14] stated that if the value of C is in the range 10^3 – 10^4 $(\Omega cm)^{-1}$, then conduction appears in the extended states, while smaller values of C indicate the presence of a wide range of localization and conduction by hopping in the localized state. Fig. 8 illustrates the relation between log ($\sigma_{DC}T$) and 1/T. If we assume that the thermal activation energy is temperature independent (like (3) implies) this plot should give a straight line, consistent with the Mott model for phonon-assisted hopping of small polarons in the adiabatic limit [15]:

$$\sigma = v_0 [e^2c(1-c)/kTR]exp(-w/kT), \quad (4)$$

where v_0 is the longitudinal optical phonon frequency, e is the electric charge, R is the average site separation, c is the fraction of sites occupied by an electron or (polaron) and w is the activation energy for DC conduction.

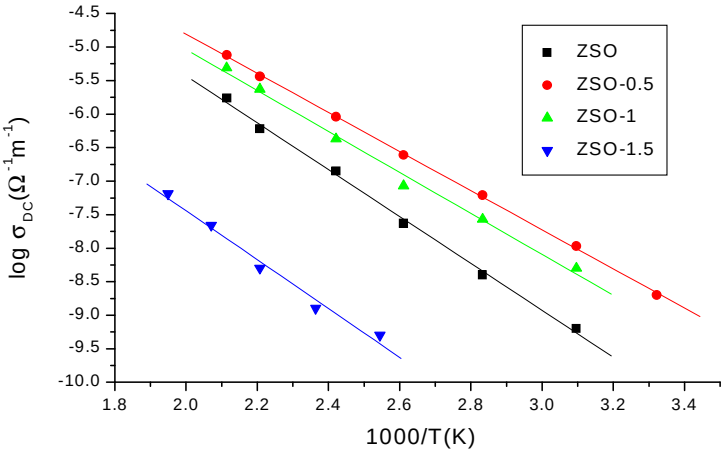

Fig. 7 Temperature dependence of the DC electrical conductivity σ_{DC}: (■, ●, ▲, ▼)

The activation energy calculated from the slope of the straight lines from Fig. 8, is w = 1.03 eV; 0.98 eV; 1.02 eV and 1.21 eV for ZSO, ZSO-0.5, ZSO-1 and ZSO-1.5, respectively, assuming that v_0 and R are constant. Imperfections in the inhomogeneous materials, such as this, caused by the fluctuations of density and/or chemical composition can be responsible for internal potential fluctuations [16] and could influence carrier movement and DC conductivity.

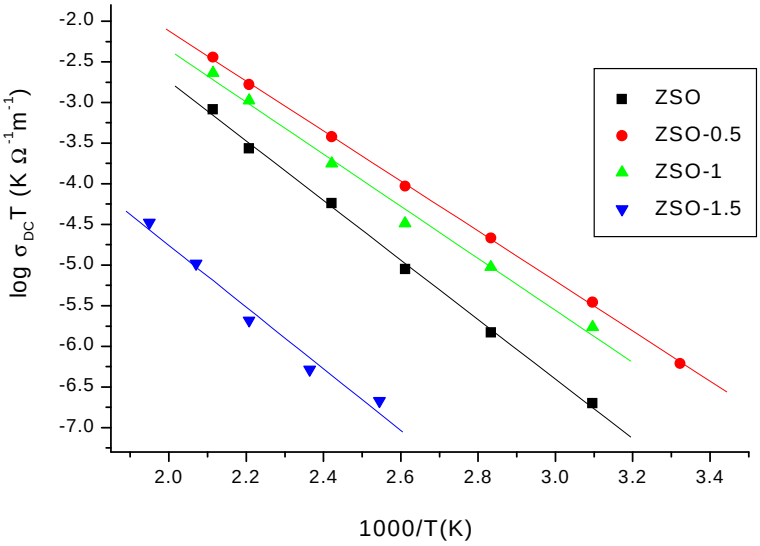

Fig. 8 The relation between log (σ_{DC}T) versus reciprocal temperature 1000/T for sintered samples: (■, ●, ▲, ▼) experimental results; (—) theoretical results calculated by Eq. (4).

Electrical conductivity over the temperature range 300K-473K, characterized by a constant activation energy, average value ~1eV, suggests that, after all, the resistivity-temperature relation could be described by a simple thermally activated hopping mechanism with a constant activation energy as predicted by equation (3).

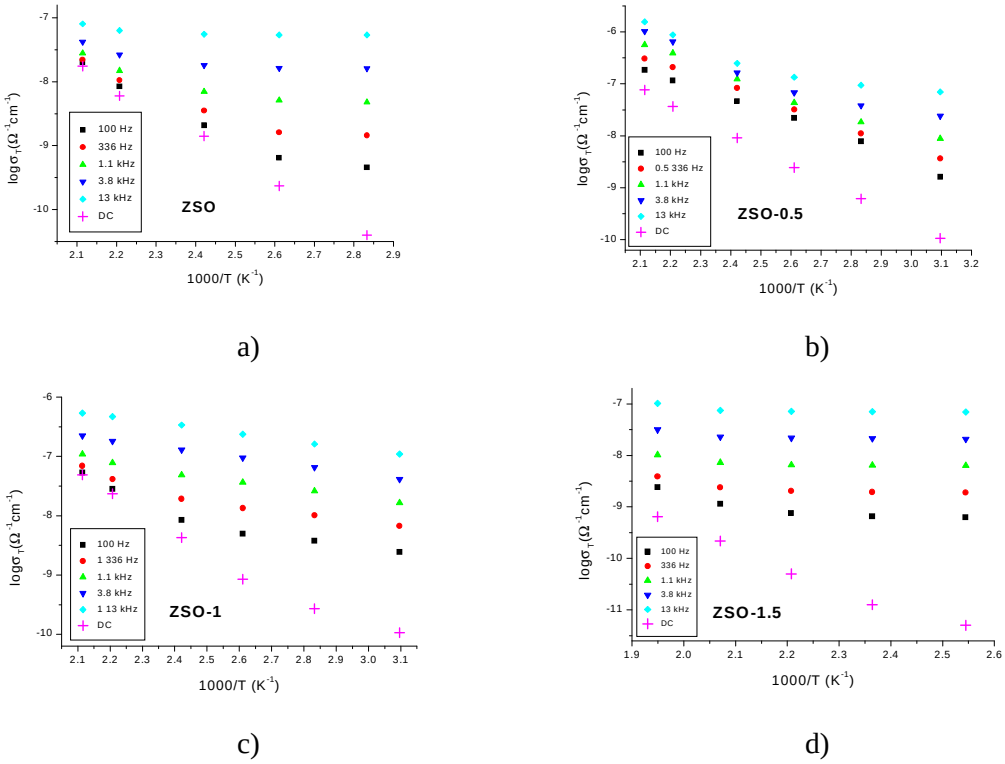

Fig. 9 Measured σ_{DC} and total conductivity σ (ω) as a function of reciprocal temperature at lower frequencies for: a) ZSO, b) ZSO-0.5, c) ZSO-1 and d) ZSO-1.5 samples.

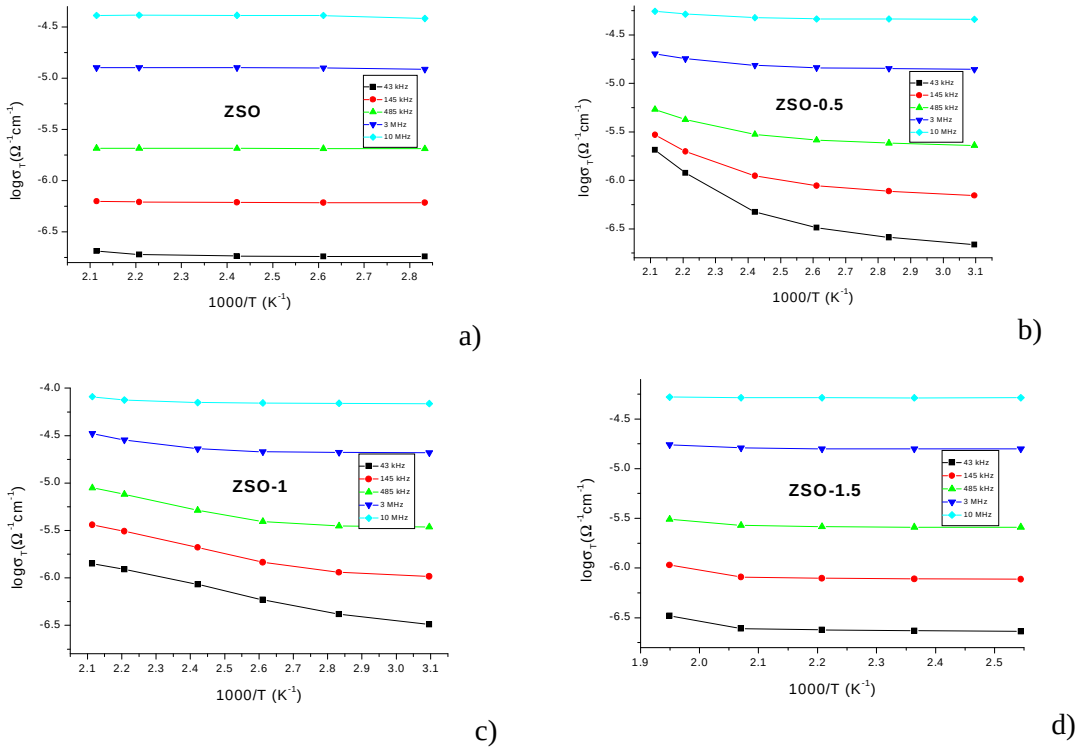

Fig. 10 Measured σ_{DC} and total conductivity σ (ω) as a function of reciprocal temperature at higher frequencies for: a) ZSO, b) ZSO-0.5, c) ZSO-1 and d) ZSO-1.5 samples.

AC conductivity

A frequency-dependent AC conductivity σ (ω) observed in many amorphous semiconductors and isolators has the form [11]:

$$\sigma_{AC}(\omega) = \sigma(\omega) - \sigma_{DC} = A\omega^{S},$$

where $\sigma_{AC}(\omega)$ is the AC conductivity, $\sigma(\omega)$ the total conductivity, σ_{DC} is the DC part of the total conductivity, A is a constant dependent on temperature, ω is the (circular) frequency and *s* is the exponent, generally less than or equal to unity.

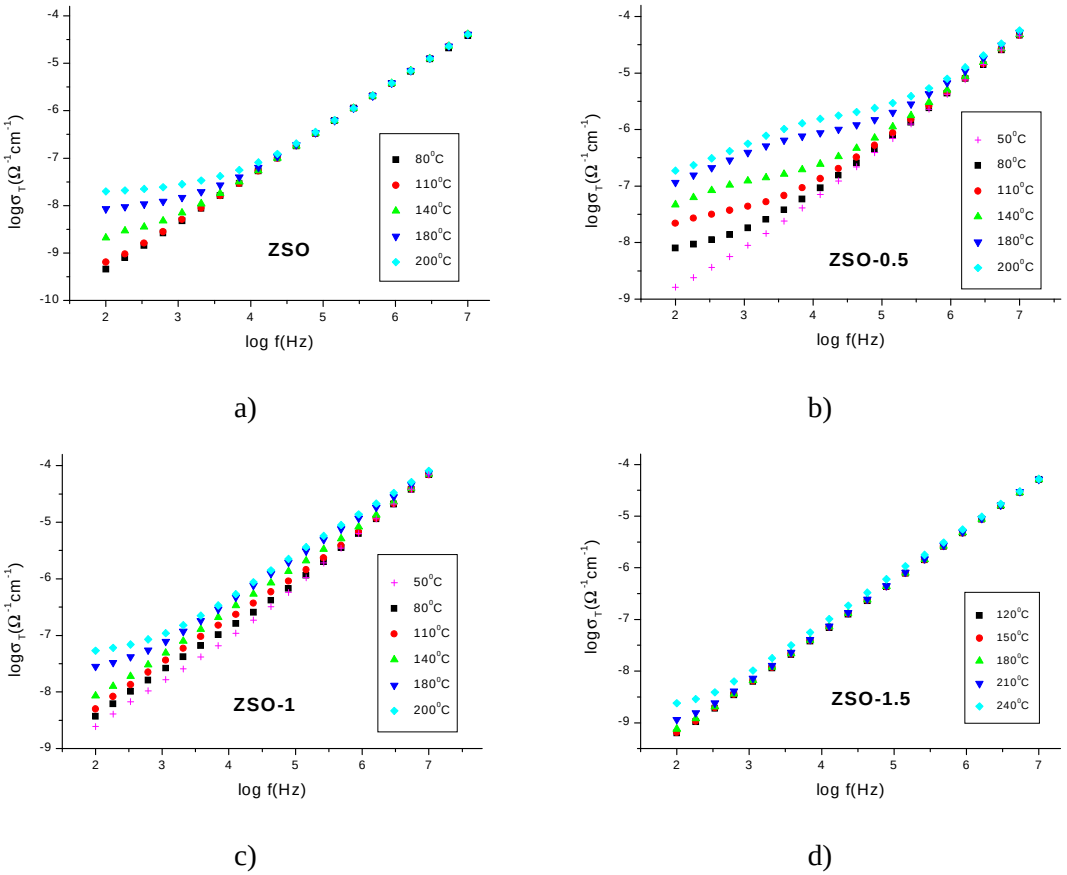

Fig. 11 Frequency dependence of the AC conductivity $\sigma_{AC}(\omega)$ at different temperatures for: a) ZSO, b) ZSO-0.5, c) ZSO-1 and d) ZSO-1.5 samples.

Frequency-dependant conductivity has been attributed to various relaxations caused by the motion of electrons or atoms and hopping or tunneling between the equilibrium sites. Fig. 9(a-d) and Fig. 10(a-d) show the measured DC and total conductivity $\sigma_T(\omega)$ as a function of reciprocal temperature at various frequencies. At lower frequencies conduction-temperature dependence is more changeable, its value increase with increase of temperature. It is evidently that the AC conductivity is higher than the DC conductivity. At higher frequencies (Fig. 10(a-d)) variation of electrical conductivity is less visibly, but obviously increases with the increase of temperature. Fig. 11 (a-d) shows the total conductivity $\sigma_T(\omega)$ versus frequency $f = (\omega/2\pi)$ at different temperatures, indicating a more gentle growth of electrical conductivity versus frequency at lower frequencies. This is particularly pronounced at higher temperatures and for samples with lower electrical conductivity such as the ZSO-0.5 sample. For the ZSO-1.5 sample, with the highest electrical resistivity, electrical conductivity increases sheerly at all frequencies and in the whole range of the observed temperatures.

Conclusion

We have studied the influence of a small addition of Bi_2O_3 to the $2ZnO\text{-}SnO_2$ system. The results strongly suggest, considering the preparation process and furthermore the addition of Bi_2O_3, that SnO_2 did not fully dissolve in the ZnO crystal lattice. The ion substitution phenomenon, reinforced by small Bi_2O_3 addition, happening between Sn^{4+} and Zn^{2+} results in the formation of a ZnO/SnO_2 solid solution with rather limited regions of pure Zn_2SnO_4. Analysis of the DC conductivity suggests carrier hopping in the localized state as the dominant conduction mechanism.

Acknowledgement

This research was performed within projects 142011G and 141026B financed by the Ministry for Science of the Republic of Serbia.

References

1. A. A. Al-Shahrani, S. Abboudy, A. W. Brinkman, J. Phys. D: Appl. Phys., 29 (1996) 2165.
2. J. H. Yu, G. M. Choi, Sens. Actuators B Chem., 72 (2001) 141.
3. J. S. Wang, S. S. Xie, Y. Gao, X. Q. Yan, D. F. Liu, H. J. Yuan, Z. P. Zhou, L. Song, L. F. Liu, W. Y. Zhou, G. Wang, J. Cryst. Growth, 267 (2004) 177.
4. R. S. Niranjan, Y. K. Hwang, D. H. Kim, S. H. Jhung, J. S. Chang, I. S. Mulla, Mater. Chem. Phys., 92 (2005) 384.
5. N. Daneu, A. Rečnik, S. Bernik, D. Kolar, J. Am. Ceram. Soc., 83 (2000) 3165.
6. V. Gil, J. Tartaj, C. Moure, P. Duran, J. Eur. Ceramic Soc., 27 (2007) 801.
7. G. Z. Zang, J. F. Wang, H. C. Chen, W. B. Su, C. M. Wang, P. Qi, Chin. Phys. Lett., 22 (2005) 750.
8. J. Wong, J. Appl. Phys., 51 (1980) 4453.
9. Y. Karakas, W. E. Lee, British Ceramic Transaction, 93 (1994) 65.
10. B. Balzer, M. Hagemeister, P. Kocher, L. J. Gauckler, J. Am. Ceram. Soc., 87 (2004) 1932.
11. H. S. Metwally, Physica B, 292 (2000) 213.
12. M. Zope, B. D. Muragi, J. K. Zope, J. Non-Cryst. Solids, 103 (1988) 195.
13. M. Fadel, A. A. Nijim, H. T. EL. Shair, Vacuum, 46 (1995) 1279.
14. N. F. Mott, Philos. Mag., 22 (1970) 7.
15. N. F. Mott, J. Non-Cryst. Solids 1 (1968) 1.
16. H. Kawazoc, H. Hosono, T. Leanazawa, J. Non-Cryst. Solids 29 (1978) 159.
17. M. Peiteado, Y. Iglesias, J. F. Fernandez, J. De Frutos, A. C. Caballero, Mater. Chem. Phys., 101 (2007) 1.

Садржај: *У овом раду испитан је утицај малог додатка (0.5; 1.0 и 1.5 мол. %) бизмут-оксида (Bi_2O_3) на микроструктуру и електрична својства цинк-калај-оксидне ($ZnO\text{-}SnO_2$) керамике. Полазни прахови ZnO и SnO_2 помешани су у моларном односу 2:1. Након додатка Bi_2O_3, ова смеша је маханички активирана десет минута у планетарном млину са куглама, пресована и синтерована на 1300ºC, два сата. Фазни састав синтерованих узорака испитан је рендгеноструктурном анализом (XRD) и енергетски-дисперзионом спектрометријом (EDS). Микроструктуре су испитане на*

скенирајућем електронском микроскопу (SEM). Импедансни спектри (100Hz – 10MHz) добијени су, на различитим температурама, уз помоћ Impedance/Gain Phase Analyzer (HP 4194A) уређаја. Електричне DC отпорности/проводности, на различитим температурама, измерене су помоћу High Resistance Meter (HP 4329A) уређаја.
Кључне речи. *Електрична својства, Микроструктура, Цинк-станат, Синтеровање.*